Bulgarian Chemical Communications, Volume 48, Number 2 (pp. 225 – 231) 2016

Room temperature acetone vapor - sensing properties of a mesoporous zinc stannate layer

I. E. Kononova[1,2], D. M. Vorobiev[1], D. Tz. Dimitrov[3]*, A. Ts. Georgieva[4], V. A. Moshnikov[1,5]

[1] *Department of Micro- and Nanoelectronics, Saint-Petersburg State Electrotechnical University, Saint-Petersburg 197376, Russia*

[2] *Department of Machines and Metal Forming Technology, Saint-Petersburg State Polytechnical University, Saint-Petersburg 195251, Russia*

[3] *Laboratory of Nanoparticle Science and Technology, Department of General and Inorganic Chemistry, Faculty of Chemistry and Pharmacy, University of Sofia, Sofia 1164, Bulgaria*

[4] *Particle Engineering Research Center, Materials Science & Engineering Department, University of Florida, Gainesville, FL 32611, USA*

[5] *Department of Integrated Electronics, Saint-Petersburg State Polytechnical University, Saint-Petersburg 195251, Russia*

Received January 13, 2015, Revised August 18, 2015

Zinc stannate porous nanostructured compositions of nanoparticles are produced in the form of thin films by means of the chemical vapor deposition method. The phase, composition and surface condition of the layers as formed by the above route are investigated. Under the application of an alternating electric field the electrical properties of the layer change under acetone vapor exposure at room temperature. As a result of this interaction the radius of the semi-circle on the Nyquist diagram is reduced and the centre of the semi-circle on the plot is shifted to the higher frequency. To describe the resistance-capacitance properties of the samples the characteristic time of charge accumulation at the atmosphere and under acetone vapor exposure is estimated. The values of the gas sensitivity in the frequency range from 1 Hz to 50 KHz is calculated in two ways based on the real and imaginary components of the complex impedance.

Keywords: nanostructures; thin films; impedance spectroscopy; surface properties.

INTRODUCTION

The gas sensors, intended for the detection of acetone in the air, are widely applied for environmental monitoring, in criminology, in military affairs, in mechanical engineering and for medical non-invasive diagnosis for the analysis of exhaled breath of patients suffering from diabetes. Now-a-days, there is still a need for the creation of nanomaterials for acetone gas sensors, operating at room temperature.

Most sensor materials show acetone vapor detection properties at elevated temperatures in the range 150–450°C [1–6]. There are only a few publications in the world literature at present, devoted to research aimed at the creation of nanomaterials that study the gas sensitive properties of acetone vapor at room temperature. These are ZnO nanorods doped with Ni, the sensitivity of which is enhanced by UV activation [7], CuO nanocrystalline thick films [8] and TiO_2 nanotubes with a certain deviation in stoichiometry [9]. To the best of our knowledge, up to now in the scientific journals there does not exist any information concerning the measurement of the complex resistivity (conductivity) of a Zinc Stannate Layer in the atmosphere under acetone vapor exposure at room temperature.

Impedance spectroscopy is a favorite tool for materials characterization, useful in gathering both, the kinetic and mechanistic information. A review of the recent progress in evaluating the gas concentration by the impedance change and the establishment of state of the art of impedance-based gas sensors is presented in [10]. Despite the well-known fact that the interaction of the material with a gaseous medium depends on the microstructure and the surface states of the sensing material, to the best our knowledge, alternating current (AC) measurement has been used for detection of gases only for a few metal oxides. The most important advantage of the alternating current (AC) measurements is that they can distinguish the individual contributions to the electrical conduction or polarization arising from different sources like the bulk and the grain boundaries, the intergranular contact regions, and the electrode-sample interface regions whereas direct current (DC) measurements show only the overall effect of all these contributions [10, 11]. It is worth mentioning that the impedance spectroscopy investigation of:

* To whom all correspondence should be sent:
E-mail: dimitrov2001@yahoo.com

undoped titanium dioxide (TiO_2) polycrystalline thin films as a function of temperature and the surrounding atmosphere are presented in [13], zirconia gas sensors [14], zeolite hydrocarbon sensors with a chromium oxide as the intermediate layer [15], room temperature gas sensing of ultrathin SnO_2 sensors prepared by the Langmuir Blodgett technique [16], WO_3 sensors sensitivity versus time and working temperature [17], $SmFeO_3$ thin-film sensor [18] and a sensing device based on vanadium oxide (V_2O_5)/porous Si /Si structure [19].

An improvement of the gas-sensitive properties can be achieved by using multi-component metal oxides as the sensor material [20–24]. Increasing the gas sensitivity is possible in principle in the case of the cooperative effect as a result of the separation of the functional properties of adsorption and complete oxidation of the reducing gases at different surface centers of the multicomponent systems. During the last few years there is a growing interest in investigations of the properties of nanostructured ZnO – SnO_2 materials, which are crystallized into perovskite ($ZnSnO_3$) [25] and spineli (Zn_2SnO_4) structures [26, 27]. The formation of such mixed oxides leads to the modification of the electronic band structure of the Zn–Sn–O system. This includes changes in the bulk and surface properties. The surface properties are expected to be influenced by new boundaries between the grains of different chemical compositions. These could be stoichiometric $ZnSnO_3$ and Zn_2SnO_4 compounds or composites. It is anticipated that all these phenomena will contribute advantageously to the gas sensing mechanism [28].

Thin films of $ZnSnO_3$ structures are very promising in the creation of new lead free ferroelectric materials [29]. Other notable applications of these nanostructured compounds are their utilization in lithium ion batteries [30], piezoelectric transformers [31], transparent conductive coatings and thin film transistors [32–34], electro-luminescence devices for power independent memory cells. Among the above applications, the number of investigations dealing with the formation of zinc stannate layers that have a highly sensing performance is increasing remarkably [35–42]. For such new generation sensing structures it is necessary to develop and evaluate the advanced technological aspects for the formation of nanostructure and nanocomposite layers, including various nanocomposits, modified nanowires, nanorods, nanospheres, nanotubes as well as nanomaterials with hierarchical porous nanostructures [43–55].

The development of three-dimensional (3D) face-centered-cubic $ZnSnO_3$ into two-dimensional (2D) orthorhombic $ZnSnO_3$ nanosheets has been observed recently [56]. The synthesis from 3D of 2D nanostructures is realized by the dual-hydrolysis-assisted liquid precipitation reaction and subsequent hydrothermal treatment. The 2D $ZnSnO_3$ nanosheets should exhibit excellent gas sensing properties of acetone vapor, especially through their ultra-fast response and recovery. The authors [56] show, that the 2D $ZnSnO_3$ nanosheets consist of smaller sized nanoflakes. This further increases the special specific surface area and facilitates their application in gas sensing.

Never-the-less, in the literature there is a hitherto unreported study devoted to the sensitivity of the $ZnSnO_3$ layer to acetone vapor at room temperature under the application of an alternating electric field. Thus, the main goal of the presented work is the formation and investigation of the surface morphology, the electrical and acetone gas sensing properties under the application of an alternative electric field at room temperature formed by a chemical vapor deposition nanosized $ZnSnO_3$ thin film.

EXPERIMENTAL

The metal oxides layers investigated in the current work are formed in a laboratory installation by means of the chemical vapor deposition (CVD) method. There are two zones inside the quartz reactor, in both of which there were boats with inorganic metal salts of tin chloride ($SnCl_2 \cdot 2H_2O$) and zinc nitrate ($Zn(NO_3)_2 \cdot 6H_2O$) while the third zone is the area of location of the holder with the substrates. The temperature required for the process is maintained in the three areas by using independent heaters. The components of the salts obtained were transferred to the deposition area in the reactor. This is done by the transfer of the vapors of volatile compounds from the areas of the tin chloride and zinc nitrate boats to the area of the holder with the substrates.

The sensing layer structures are formed by using three subsequent processes:

- Decomposition of tin chloride ($SnCl_2 \cdot 2H_2O$) and zinc nitrate ($Zn(NO_3)_2 \cdot 6H_2O$) at the temperature of 150 °C under an air flow within the quartz reactor;
- After decomposition within the quartz reactor the reaction products are transferred to the substrates;
- The formation of the $ZnSnO_3$ layer at the temperature of 500 °C from the transferred to the substrate reaction products;

Thermally oxidized silicon was used as a substrate. The thickness of the oxide layer was about 500 nm. Before application the substrates were treated in acetone and isopropyl alcohol in an ultrasonic bath. The thickness of the $ZnSnO_3$ layers, deposited on the substrates is about 500 nm, estimated by means of ellipsometry measurements.

The investigations of the phase composition of layers formed by the above route are done on a low angle registration electron-diffraction apparatus (SELMI, Ukraine). Electron diffraction [57, 58] is a local (small extinction length) an express (high intensity particle flux) method of structural analysis. The method of electron diffraction is indispensable in the study of near-surface regions, thin films and other nano-objects. The investigation is evaluated by comparison of the diffraction patterns of nonelastically scattered electrons in refraction geometry.

The conductive substrate necessitates the determination of its phase composition by means of a low-angle registering electronograph. Because of this electron diffraction experiments were performed on $ZnSnO_3$ layers deposited on a non-oxidized silicon substrate. However, to investigate the gas-sensing properties of the $ZnSnO_3$ layers it was necessary to deposit these on an oxidized silicon substrate. Silicon oxide is an insulating dielectric layer between the silicon and the semiconductor layer of zinc stannate. It was used to avoid the conductive silicon and contributes to the gas sensing properties of zinc stannate.

The investigation of the surface condition of the nanostructured film formed by oxidation of a silicon dielectric layer is done on a nanolaboratory instrument Ntegra Terma (NT-MDT, Zelenograd). It was performed by means of a “semi-contact” vibrational AFM mode. Probe type sensors with cantilevers series NSG 01 in the form of a rectangular cross-section rafter were used in the investigation. This has a resonance frequency of 150 кHz and was purchased from the NT-MDT Company.

The electrical properties of $ZnSnO_3$ nanostructures are studied by means of impedance spectroscopy measurments. It is well know that this method is widely used to investigate the electrical properties of the grain boundary under the application of an electrical field with an alternative frequency. Measuring the frequency dependences of the complex resistivity modulus and determination of the phase shift angle between the current and voltage in the capacitance circuit were carried out in the frequency range between 1 Hz to 500 kHz with an amplitude of the alternating voltage equal to 30 mV. On our experimental setup [59] we were able to measure the electrical properties of the nanostructure at the atmosphere and under exposure to acetone vapor in the air. The concentration of acetone was 100, 200 and 300 ppm and at a relative humidity of 80 %.

RESULTS OF THE INVESTIGATION OF THE STRUCTURAL PROPERTIES OF MESOPOROUS $ZnSnO_3$ LAYERS AND THEIR SENSING PERFORMANCE UNDER THE APPLICATION OF AN ALTERNATING ELECTRIC FIELD

The result of electron diffraction for the zinc stannate layer, deposited on an oxide free silicon wafer is shown on Fig.1. It presents the typical dependence of the signal intensity on the photoelectron multiplier as a function of the interplanar distance d. The latter is calculated based on the value of the distance from the central spot. The diffraction peaks for nonelastic scattered electrons, corresponding to the crystallized in perovkside structure nanosructured phase of $ZnSnO_3$ are marked by solid dots. It is clear, that under the applied technological conditions of chemical vapor deposition, the corresponding $ZnSnO_3$ crystal phase exhibits only reflections. An electron diffraction image for the same sample is presented in Fig.2.

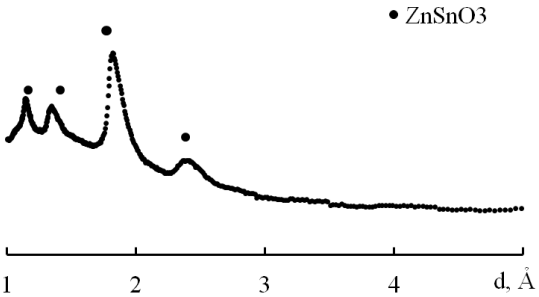

Fig. 1. Cross-section of electron diffraction pattern at radius from the central spot toward the interplanar distance d for the based on ZnSnO3 layer.

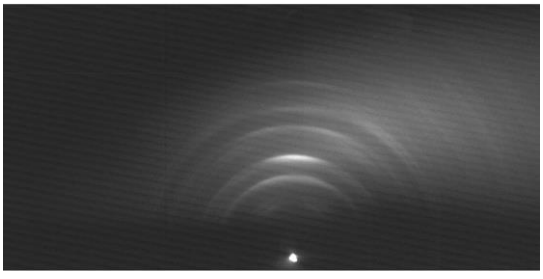

Fig. 2. Electron-diffraction image for the based on $ZnSnO_3$ layer.

In the current work the AFM images were in the form of a square matrix with the size 256×256 of

the elements. Based on the AFM investigation it was estimated that the produced nanostructured materials are an aggregation of nanoparticles with sizes in the range of 10-100 nm. Into the matrix of the nanoparticles, the pores in size less than 10nm are uniformly distributed. An example for a typical $ZnSnO_3$ nanostructure, deposited on the substrate of oxidized silicon is presented on Fig.3 for a scanning area of $1\mu m \times 1\mu m$.

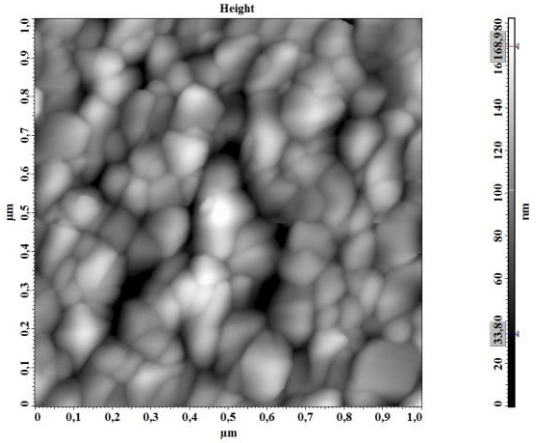

Fig. 3. AFM image of ZnSnO3 layer

The experimental data measured by means of impedance spectroscopy were evaluated by using a complex plane on which the impedance value and other complex quantity is presented in the form of a dependence of the real and imaginary component of the complex resistivity. The frequency dependences of the real and imaginary components of the complex resistivity for the $ZnSnO_3$ nanostructure are plotted in semi-logarithmic coordinates and analyzed. It was revealed that the imaginary component of the complex resistivity is going through a maximum when $\omega\tau=1$, where ω is the angular frequency and τ the time of the relaxation polarization. Nyquist diagrams for the nanostructured $ZnSnO_3$ layer at the atmosphere and under acetone vapor exposure (100, 200, 300 ppm) at room temperature were presented in Fig.4.

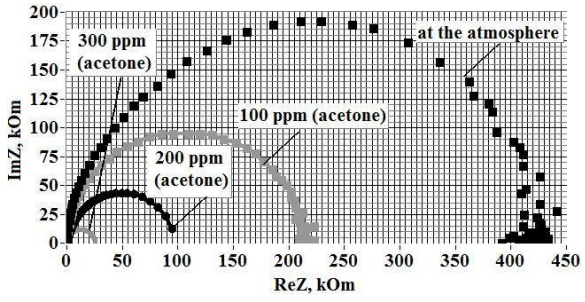

Fig. 4. Nyquist diagram for the nanostructured $ZnSnO_3$ layer at the atmosphere and under various concentrations of acetone vapour exposure.

DISCUSSION

Basic working principle of operation of the solid state gas sensors is the alternation of semiconductive oxide layer electrical properties under adsorption of gas molecules. Atoms or molecules adsorbed on the nanostructured oxide surface can capture electrons from or inject electrons into the bulk to form localized electron extrinsic energy state at the surface, which can change the concentration of charge carriers into conduction band or valence band. It is known that acetone is an electron-donor molecule, which has two electron pairs on highest occupied molecular orbital (HOMO), which can be donated to form coordinate bond. The lone pairs are relatively high in energy, and are responsible for the well known Lewis base properties of acetone. When the sensor is exposed to acetone vapor, the gas molecules are adsorbed on the surface of the gas-sensing layer and the weak coordinate bonds can be formed between acetone and Sn (IV) ions from the $ZnSnO_3$ crystal lattice. Similar interaction is in the case when the PbS sensor is exposed to NO_2 or NH_3 gas. Then the gas molecules are adsorbed on the surface of the gas-sensing layer and the weak coordinate bonds is formed between NO_2 or NH_3 and lead(II) in PbS molecules [60]. In our case, electrons are transferred from acetone molecules to the gas-sensing layer and the thickness of surface space depletion layer at the grain boundary of $ZnSnO_3$ crystallites will be decreased. This will modulate conductive channels at the contacts of the nanocrystalites. The molecules of acetone will interact with oxygen, which is unavoidable existing on $ZnSnO_3$ crystallites and adsorb there according to the reaction below:

$$O_{2\,gas} + e^- + [S] \rightarrow O_2^-$$

where $O_{2\,gas}$ - oxygen molecule in the atmosphere, e^- - free electron at the $ZnSnO_3$ crystallites surface, $[S]$ - unoccupied center for oxygen chemisorptions, O_2^- - adsorbed on the surface one charged oxygen molecule. Acetone adsorbed on the surface, reacts with the above mentioned molecular oxygen ions and captured by it electrons are released into the layer, according to the reaction:

$$CH_3COCH_3 + 4O_2^- \rightarrow 3CO_2 + 3H_2O + 4e^-$$

By this way, no matter that adsorption of one acetone molecule provides two electrons to the $ZnSnO_3$ layer, after its oxidation four electrons are released into the layer. Consequently, after oxidation of the adsorbed acetone the total effect is

increasing the conductivity of the layer. Under acetone vapor exposure the radius of the semi-circle on the Nyquist diagram is reduced (Fig. 4) and the centre of semi-circle on the plot is shifted to the higher frequency. The reason for this effect is the relaxation maximum shift of the imaginary component of complex resistivity to the area of higher frequencies.

The equivalent electric scheme is used for interpretation of observed capacitance-resistance properties of nanostructured $ZnSnO_3$ layer. A constant phase element, widely used for modeling impedance of many electrical systems was employed. This scheme describes well the exponential dependence of parameters of chemical-physics processes, related to overcoming energy threshold during the charge transfer and impedance behavior. Also, the scheme is connected to the appearing of fractal properties of investigated structures in particular frequency range. Impedance of the element with constant phase is described by equation: $Z = 1/A(j\omega)^n$, where A - proportionality factor, j - the imaginary unit, n- exponent index, giving the information about the phase shift, $-1 \le n \le 1$. Frequency independent factor has physical meaning and dimension of capacitance.

The plotted on Fig.4 impedance hodographs are evaluated for the circuit, constructed of connected in parallel resistance R and the constant phase component. This circuitry can be characterized by resistance and constant phase component of the grain boundary of $ZnSnO_3$ crystallites. The hodographs consist of semi-circles with center below the horizontal axis. The characteristic time of charge accumulation for the circuit, constructed from connected in parallel resistance R and the constant phase component is expressed by equation $\tau = (R \cdot A)^{1/n} = 1/\omega$, where ω is angular frequency at the point where imaginary component of complex resistivity having maximum value (at the point of relaxation maximum on impedance hodograph).

Let's consider the impedance hodographs in air and in the presence of acetone vapor with concentration of 100 ppm. Values of resistivity R, frequency independent fore-exponential factor A, exponent index n, relaxation maximum frequency f_{max} and time of relaxation polarization τ at the atmosphere and under acetone vapor exposure are calculated. It was revealed that under acetone vapor exposure value of resistivity R is reduced by factor of 1.99; value of frequency independent fore-exponential factor A is reduced by factor of 1.39; value of relaxation maximum frequency f_{max} is increases by factor of 2.89. It was found that under acetone vapor exposure value of exponent index n is not changed and is 0.94; value of time of relaxation polarization τ is 184 μsec in the atmosphere and 64 μsec under acetone vapor exposure.

Based on the above investigations, the value of gas-sensitivity is evaluated in two ways: (i) by the real component of the complex resistivity as $S_{Re} = ReZ_{air} / ReZ_{gas}$, where ReZ_{air} is the real component of the complex resistivity at the atmosphere, ReZ_{gas} is the real component of the complex resistivity under acetone vapor exposure; (ii) by the imaginary component of the complex resistivity as $S_{Im} = ImZ_{air} / ImZ_{gas}$, where ImZ_{air} is the imaginary component of complex resistivity at the atmosphere, ImZ_{air} – is the imaginary component of the complex resistivity under acetone vapor exposure. The estimated value of sensitivity is 2.0, calculated by real component and is 4.2 while calculated by imaginary component. It was revealed that in both cases the maximum of the sensitivity toward acetone vapor is at frequency low than 140 Hz.

Because in the World wide literature to the best of our knowledge does not exist any results of investigation of complex resistivity (conductivity) of Zinc Stannate Layer at the atmosphere and under acetone vapor exposure at room temperature we cannot compare the functional properties of the produced in this work films with similar films of the scientific periodic. At the available literature existing only done at direct current (DC) measurements of gas-sensitive properties of Zinc Stannate Layers [37, 38, 40, 41, 56].

CONCLUSIONS

In this work is presented the procedure of producing zinc stannate based porous nanostructured composition by chemical vapor deposition method. The produced layers are composed from aggregations of nanoparticles 10-100 nm in size. Into the nanoparticles matrix pores are regularly distributed. Under application of alternative electric field the electrical properties of the layer change under acetone vapor exposure at room temperature. Under acetone vapor exposure the radius of the semi-circle on the Nyquist diagram is reduced and the centre of semi-circle on the plot is shifted to the higher frequency. The reason for this effect is the relaxation maximum shift of the

imaginary component of complex resistivity to the area of higher frequencies.

Acknowledgments: *D. Dimitrov is thankful for financial support to the Beyond Everest project FP7-REGPOT-2011-1. The Russian researchers are thankful to the grant of Russian Scientific Fund (project №14-15-00324). The authors are grateful to both Dr. Kamilu Gazinyrovich Gareev for help in investigation the phase composition of the nanostructures by electron diffraction measurements.*

REFFERENCES

1. L. Wang, A. Teleki, S. Pratsinis, P. Gouma, *Chem. Mater.*, **20**, 4794 (2008).
2. K.W. Kao, M.-Ch. Hsu, Yu.-H. Chang, Sh. Gwo, J. A. Yeh, *Sens.*, **12**, 7157 (2012).
3. P. Yu, J. Wang, H.-Yi Du, P.-J. Yao, Y. Hao, X.-G. Li, *J. Nanomater.*, **2013**, 1 (2013).
4. H. Shan, Ch. Liu, L. Liu, Sh. Li, L. Wanga, X. Zhang, X. Bo, X. Chi, *Sens. Actuators B*, **184**, 243 (2013).
5. Yi. Zhang, W. He, H. Zhao, P. Li, *Vacuum*, **95**, 30 (2013).
6. X. B. Li, S. Y. Ma, F. M. Li, Y. Chen, Q. Q. Zhang, X. H. Yang, C. Y. Wang, J. Zhu, *Mater. Lett.*, **100**, 119 (2013).
7. H. Ahn, Y. Wang, S. H. Jee, M. Park, Y. S. Yoon, D.-J. Kim, *Chem. Phys. Lett.*, **511**, 331 (2011).
8. I. Singh, R. K. Bedi, *AIP Conf. Proc.*, **1536**, 1175 (2013).
9. B. Bhowmik, A. Hazra, K. Dutta, P. Bhattacharyya, Device and Materials Reliability, *IEEE Transact.* **PP 99**, 1 (2014).
10. J. M. Rheaume, A. P. Pisano, *Ionics*, **17**, 99 (2011).
11. J. R. Macdonald, *Ann. Biomed. Eng.*, **20**, 289 (1992).
12. O. K. Varghese, L. K. Malhotra, *J. Appl. Phys.*, **87**, 7457 (2000).
13. M. A. Ponce, R. Parra, R. Savu, E. Joanni, P. R. Bueno, M. Cilense, J. A. Varela, M. S. Castro, *Sens. Actuators B*, **139**, 447 (2009).
14. S. Zhuiykov, Electrochemistry of Zirconia Gas Sensors, Taylor Francis Group, USA, 2007.
15. G. Hagen, A. Schulz, M. Knörr, R. Moos, *Sensors (Basel*, **7**, 2681 (2007).
16. C. A. Betty, S. Choudhury, K. G. Girija, *Sens. Actuators B*, **173** 781 (2012).
17. A. Abidi, C. Jacolin, M. Bendahan, A. Abdelghani, J. Guerin, K. Aguir, M. Maaref, *Sens. Actuators B*, **106**, 713 (2005).
18. T. Tasaki, S. Takase, Y. Shimizu, *J. Sens. Tech.*, **2**, 75 (2012).
19. K. Chebout, A. Iratni, A. Bouremana, K. M'hammedi, H. Menari, A. Keffous, N. Gabouze, The Third International Conference on Sensor Device Technologies and Applications, SENSORDEVICES 2012, Rome, Italy, 2012, p.42.
20. E. H. Espinosa, R. Ionescu, B. Chambon, G. Bedis, E. Sotter, C. Bittencourt, A. Felten, J.-J. Pireaux, X. Correig, E. Llobet, *Sens. Actuators B*, **127**, 137 (2007).
21. G. Lu, J. Xu, J. Sun, Y. Yu, Y. Zhang, F. Liu, *Sens. Actuators B* , **162**, 82 (2012).
22. Y. Gui, S. Li, J. Xu, C. Li, *J. Microelectr.*, **39**, 1120 (2008).
23. D. R. Patil, L. A. Patil, P. P. Patil, *Sens. Actuators B*, **126**, 368 (2007).
24. G. Korotcenkov, Handbook of Gas Sensor Materials: Properties, Advantages and Shortcomings for Applications Volume 1: Conventional Approaches, Springer, 2013.
25. B. Geng, C. Fang, F. Zhan, N. Yu, *Small*, **4**, 1337 (2008).
26. Z. Li, Y. Zhou, C. Bao, G. Xue, J. Zhang, J. Liu, T. Yu, Z. Zou, *Nanoscale*, **4**, 3490 (2012).
27. S. Baruah, J. Dutta, *Sci. Technol. Adv. Mater.*, **12**, 01300410 (2011).
28. K. Zakrzewska, *Thin Solid Films*, **391**, 229 (2001).
29. J. Y. Son, G. Lee, M.-H. Jo, H. Kim, H. M. Jang, Y.-H. Shin, *J. Am. Chem. Soc.*, **131**, 8386 (2009).
30. Z. Y. Yuan, F. Huang, J. T. Sun, Y. H. Zhou, *Chem. Lett.*, **31**, 408 (2002).
31. J. M. Wu, C. Xu, Y. Zhang, Z. L. Wang, *ACS Nano*, **6**, 4335 (2012).
32. Y.-J. Chang, D.-H. Lee, G. S. Herman, C.-H. Chang, *Electrochem. Solid-State Lett.*, **10**, H135 (2007).
33. C.-G. Lee, A. Dodabalapur, *Appl. Phys. Lett.*, **96**, 2435011 (2010).
34. S.-J. Seo, C. G. Choi, Y. H. Hwang, B.-S. Bae, *J. Phys. D*, **42**, 0351061 (2009).
35. S. An, C. Jin, H. Kim, S. Lee, B. Jeong, C. Lee, *Nano*, **7**, 12500131 (2012).
36. A. Sivapunniyam, N. Wiromrat, M. T. Z. Myint, J. Dutta, *Sens. Actuators B*, **157**, 232 (2011).
37. B. C. Yadav, R. Singh, S. Singh, P. K. Dwivedi, *Intern. J. Green Nanotechn.*, **4**, 37 (2012) .
38. J. Huang, X. Xu, C. Gu, W. Wang, B. Geng, Y. Sun, J. Liu, *Sens. Actuators B*, **171–172**, 572 (2012).
39. H. Fan, Y. Zeng, X. Xu, N. Lv, T. Zhang, *Sens. Actuators B*, **153**, 170 (2011).
40. P. Song, Q. Wang, Z. Yang, *Sens Actuators B*, **156**, 983 (2011).
41. Y. Zeng, K. Zhang, X. Wang, Y. Sui, B. Zou, W. Zheng, G, Zou, *Sens. Actuators B*, **159**, 245 (2011).
42. W. Zeng, T. Liu, Z. Wang, *Mater. Transact.*, **51**, 1326 (2010).
43. W. Zhang, C. Zeng, M. Kong, Y. Pan, Z. Yang, *Sens. Actuators B*, **162**, 292 (2012).
44. H. Men, P. Gao, B. Zhou Y. Chen, C. Zhu, G. Xiao, L. Wanga, M. Zhang, *Chem. Commun.*, **46**, 7581 (2010).
45. J. Chen, L. Lu, W. Wang, *J. Phys. Chem. C*, **116**, 10841 (2012).
46. R. Acharya, Y. Q. Zhang, X. A. Cao, *Thin Solid Films*, **520**, 6130 (2012).
47. K. Saravanakumar, K. Ravichandran, R. Chandramohan, S. Gobalakrishnanc, M. Chavalic, *Superlatt. Microstr.*, **52**, 528 (2012).

48. V. A. Moshnikov, I. E. Gracheva, V. V. Kuznezov, A. I. Maximov, S. S. Karpova, A. A. Ponomareva, *J. Non-Cryst. Solids*, **356**, 2020 (2010) .
49. I. E. Gracheva, V. A. Moshnikov, S. S. Karpova, E. V. Maraeva, *J. Phys. Conf. Ser.*, **291**, 0120171 (2011).
50. I. E. Gracheva, Y. M. Spivak, V. A. Moshnikov, AFM techniques for nanostructures materials used in optoelectronic and gas sensors, IEEE Eurocon-2009, Saint-Petersburg, 2009, p.1250.
51. I. E. Gracheva, V. A. Moshnikov, E. V. Maraeva, S. S. Karpova, O. A. Alexsandrova, N. I. Alekseyev, V. V. Kuznetsov, G. Olchowik, K. N. Semenov, A. V. Startseva, A. V. Sitnikov, J. M. Olchowik, *J. Non-Cryst. Solids*, **358**, 433 (2012) .
52. V. A. Moshnikov, I. E. Gracheva, M. G. An'chkov, *Glass Phys. Chem.* , **37**, 485 (2011).
53. A. A. Ponomareva, V. A. Moshnikov, G. Suchaneck, *Mater. Sci. Eng.*, **30** , 0120031 (2012).
54. V. A. Moshnikov, I. E. Gracheva, A. S. Lenshin, Y. M. Spivak, M. G. Anchkov, V. V. Kuznetsov, J. M. Olchowik, *J. Non-Cryst. Solids*, **358**, 590 (2012).
55. N. V. Kaneva, D. T. Dimitrov, C. D. Dushkin, *Appl. Surf. Sci.*, **257**, 8113 (2011).
56. Y. Chen, L. Yu, Q. Li, Y. Wu, Q. Li, T. Wang, *Nanotech.* , **23**, 415501 (2012).
57. L. H. Germer, *Phys. Rev.*, **56**, 58 (1939).
58. A. K. Srivastava, R. Kishore, S. A. Agnihotry, *Indian J. Eng. Mater. Sci.*, **11**, 315 (2004).
59. I. E. Gracheva, V. A. Moshnikov, M. G. An'chkov, *Instrum. Exper. Tech.*, **56**, 209 (2013).
60. T. Fu, *Sens. Actuators B*, **140**, 116 (2009).

ОПРЕДЕЛЯНЕ ПРИ СТАЙНА ТЕМПЕРАТУРА НА СЕНЗОРНИТЕ СВОЙСТВА НА МЕЗОПОРЕСТ СЛОЙ ОТ ЦИНКОВ СТАНАТ ПО ОТНОШЕНИЕ НА ИЗПАРЕНИЯ НА АЦЕТОН

И. Е. Кононова [1,2], Д. М. Воробьов[1], Д. Ц. Димитров[3]*, А. Ц. Георгиева[4], В. А. Мошников[1,5]

[1] Катедра по Микро- и Наноелектроника, Санкт-Петербургски държавен електротехнически университет, Санкт-Петербург 197376, Русия

[2] Катедра по Машини и технологии за формиране на метални детайли, Санкт-Петербургски държавен политехнически университет, Санкт Петербург 195251, Русия

[3] Лаборатория за Наука и технология на наночастици, Катедра по Обща и неорганична химия, Факултет по Химия и фармация, Софийски университет, София 1164, България

[4] Инженерен изследователски центъра за изследване на свойствата на елементарните частици, Катедра по Материалознание и инженерни науки, Университет на Флорида, Гейнсвил, Флорида 32611, САЩ

[5]Катедра по Интегрална електроника, Санкт-Петербургски държавен политехнически университет, Санкт Петербург 195251, Русия

Получена на 13 януари 2015, Преработена на 18 август 2015

(Резюме)

Цинк станатни порьозни наноструктурирани композиции от наночастици са получени под формата на тънки слоеве посредством метода химическо отлагане от изпарения. На формираните по гореспоменатия начин слоеве са изследвани фазовия състав и състоянието на повърхността. При прилагане на променливо електрическо поле електрическите характеристики на слоя се измененят под въздействие на изпарения от ацетон при стайна температура. Като резултат на това взаимодействие радиуса на полукръга на диаграмата Найкуист се намалява и центъра на полукръга на графиката се измества към по-висока честота. При описване на резистивно-емкостните свойства на пробите се оценява характерното време на акумулиране на заряд на въздушна атмосфера и при излагане на ацетонови изпарения. Стойностите на чувствителността към изпарения на ацетон в честотния обхват от 1 Hz до 50KHz са изчислени по два начина на базата на реални и имагинерни компоненти на комплексния импеданс.